Circulation

ORIGINAL RESEARCH ARTICLE

The N^6-Methyladenosine mRNA Methylase METTL3 Controls Cardiac Homeostasis and Hypertrophy

Editorial, see p 546

Lisa E. Dorn, BA
Lior Lasman, BMS
Jing Chen, PhD
Xianyao Xu, MS
Thomas J. Hund, PhD
Mario Medvedovic, PhD
Jacob H. Hanna, MD, PhD
Jop H. van Berlo, MD, PhD
Federica Accornero, PhD

BACKGROUND: *N*^{6}-Methyladenosine (m6A) methylation is the most prevalent internal posttranscriptional modification on mammalian mRNA. The role of m6A mRNA methylation in the heart is not known.

METHODS: To determine the role of m6A methylation in the heart, we isolated primary cardiomyocytes and performed m6A immunoprecipitation followed by RNA sequencing. We then generated genetic tools to modulate m6A levels in cardiomyocytes by manipulating the levels of the m6A RNA methylase methyltransferase-like 3 (METTL3) both in culture and in vivo. We generated cardiac-restricted gain- and loss-of-function mouse models to allow assessment of the METTL3-m6A pathway in cardiac homeostasis and function.

RESULTS: We measured the level of m6A methylation on cardiomyocyte mRNA, and found a significant increase in response to hypertrophic stimulation, suggesting a potential role for m6A methylation in the development of cardiomyocyte hypertrophy. Analysis of m6A methylation showed significant enrichment in genes that regulate kinases and intracellular signaling pathways. Inhibition of METTL3 completely abrogated the ability of cardiomyocytes to undergo hypertrophy when stimulated to grow, whereas increased expression of the m6A RNA methylase METTL3 was sufficient to promote cardiomyocyte hypertrophy both in vitro and in vivo. Finally, cardiac-specific METTL3 knockout mice exhibit morphological and functional signs of heart failure with aging and stress, showing the necessity of RNA methylation for the maintenance of cardiac homeostasis.

CONCLUSIONS: Our study identified METTL3-mediated methylation of mRNA on *N*^{6}-adenosines as a dynamic modification that is enhanced in response to hypertrophic stimuli and is necessary for a normal hypertrophic response in cardiomyocytes. Enhanced m6A RNA methylation results in compensated cardiac hypertrophy, whereas diminished m6A drives eccentric cardiomyocyte remodeling and dysfunction, highlighting the critical importance of this novel stress-response mechanism in the heart for maintaining normal cardiac function.

Key Words: gene expression profiling ■ hypertrophy ■ mice, transgenic ■ RNA processing, post-transcriptional

Sources of Funding, see page 544

© 2018 The Authors. *Circulation* is published on behalf of the American Heart Association, Inc., by Wolters Kluwer Health, Inc. This is an open access article under the terms of the Creative Commons Attribution Non-Commercial License, which permits use, distribution, and reproduction in any medium, provided that the original work is properly cited and is not used for commercial purposes.

https://www.ahajournals.org/journal/circ

ORIGINAL RESEARCH ARTICLE

Clinical Perspective

What Is New?

- We discovered that methylation at the N^6-Methyladenosine (m6A), the most abundant mRNA modification, is increased under hypertrophic conditions in cardiomyocytes and enriched on genes involving protein kinases and intracellular signaling pathways, suggesting a regulatory role in the cardiac hypertrophic pathway.
- Increasing the expression of the m6A methyltransferase-like 3 (METTL3) in the heart drives spontaneous, compensated hypertrophy but does not affect cardiac function, whereas METTL3 knockdown induces maladaptive eccentric remodeling and leads to morphological and functional signs of heart failure.
- METTL3, through m6A, helps modulate cardiac homeostasis and hypertrophic stress responses in mice.

What Are the Clinical Implications?

- Our study demonstrates the importance of METTL3 and m6A modulation throughout the heart's lifespan, both in terms of cardiac homeostasis with aging and the heart's response to pressure-overload stress.
- Our data determine that perturbing METTL3 and m6A levels induces spontaneous geometric changes in cardiomyocytes, thereby determining the adaptive or maladaptive nature of the resulting cardiac remodeling.
- Targeting m6A through its writer enzyme METTL3 may represent a novel therapeutic strategy for managing maladaptive cardiac hypertrophy and remodeling during the progression of heart failure.

The heart comprises long-lived cardiomyocytes that, in response to stress stimulation such as pressure overload or myocardial infarction, undergo hypertrophic growth. This hypertrophic response is initially an adaptive process to produce sufficient force to match an increase in wall tension or increased workload, but can ultimately lead to heart failure.[1] Cardiac hypertrophy is mediated by increased gene expression and production of select proteins in cardiomyocytes.[2] In the past, many studies have focused on the signaling pathways leading to activation of prohypertrophic transcription factors that selectively augment gene expression in the heart.[3] Although significant progress has been made in understanding the transcriptional control of gene expression during hypertrophy, it is now clear that posttranscriptional regulation of protein expression is a similarly critical mechanism for hypertrophic control.[4] For example, RNA splicing factors and microRNA-mediated gene silencing are established mechanisms of posttranscriptional regulation of gene expression that directly alter protein levels in the heart.[5–7] However, the extent to which modifications of the mRNA itself can regulate cardiac hypertrophy is not known.

The most abundant internal mRNA posttranscriptional modification is methylation at the N^6-Methyladenosine (m6A), a modification catalyzed by the enzyme methyltransferase-like 3 (METTL3).[8–10] m6A mRNA modification adds a new dimension to the developing landscape of posttranscriptional regulation of gene expression. It is now clear that m6A methylation plays important and diverse biological functions in plants, yeast, flies, and mammals.[11–16] For example, m6A manipulation via knockdown or deletion of METTL3 affects plant growth, yeast meiosis, body mass and metabolism, synaptic signaling, circadian clock regulation, and stem cell self-renewal and differentiation.[11–16] Despite the growing appreciation of the biological significance of mRNA methylation, the mechanisms by which m6A might regulate gene expression are complex and appear to be context- and cell type–dependent.

Although m6A mRNA methylation has long been recognized as a posttranscriptional modification in mammalian cells, the roles of this posttranscriptional process and the functions of m6A mRNA methylation in cardiomyocytes and in animal models of cardiac function are completely unknown. Here, we identified the m6A mRNA methylation sites in cultured cardiomyocytes, and show that inhibition of the methylase METTL3 blocks hypertrophy. We also found that reduction of m6A levels by deleting METTL3 in cardiomyocytes leads to long-term loss of normal cardiac structure and function in vivo. Conversely, enhancing m6A mRNA methylation in cardiomyocytes promotes spontaneous hypertrophic cardiomyocyte growth that results in compensated cardiac remodeling.

METHODS

All data, material and methods are available on request. RNA sequencing data are accessible at the Gene Expression Omnibus database as also specified below.

Animals

The generation of Mettl3 loxP-targeted (fl) mice (Mettl3 fl/fl) was previously described.[12] Mettl3 fl/fl mice were crossed with mice expressing cre recombinase under the control of the cardiac-specific Myh7 promoter (β-myosin heavy chain [β-MHC]) to obtain heart-restricted deletion of Mettl3 (METTL3-cKO; cKO). Control mice for this group are $Mettl3^{+/+}$ β-MHC cre. METTL3-cKO and control mice are on a C57BL6 background. A tetracycline/doxycycline-responsive binary α-myosin heavy chain (α-MHC) transgene system was used to express METTL3 in cardiomyocytes. This responder line was crossed with cardiac-restricted α-MHC transgenic mice expressing the tetracycline transactivator protein (all in the FVB/N background) to generate an overexpression

transgenic system (METTL3-TG; M3-TG; TG). Controls for this group are tetracycline transactivator single transgenic mice. Male and female mice, 10 to 32 weeks old, were used in this study. Echocardiographic measurements were taken using a Vevo2100 Visual Sonics (Visual Sonics) system and MS-400 transducer. The mice were lightly anesthetized (1.5% isoflurane) and the ejection fraction, fractional shortening, and ventricular chamber dimensions were determined in the M-mode using the parasternal short-axis view at the level of the papillary muscles. Ejection fraction, fractional shortening, ventricular chamber dimensions, left ventricular mass, and heart rate were calculated automatically using the VevoLAB program. Relative wall thickness (RWT) was calculated using the formula $RWT = \frac{2 * LVPWd}{LVIDd}$, where LVPWd indicates left ventricular posterior wall dimension end diastole, and LVIDd indicates left ventricular internal diameter end diastole. All echocardiographic measurements are reported in Table I in the online-only Data Supplement. Cardiac injury was induced by transverse aortic constriction to produce pressure overload. In short, the transverse aortic arch was visualized through a median sternotomy, and a 7-0 silk ligature was tied around the aorta using a 27-gauge wire to obtain a defined degree of constriction between the right brachiocephalic and left common carotid arteries. Infusion of angiotensin II (432 μg/kg of body weight/d) and phenylephrine (100 $mg \cdot kg^{-1} \cdot d^{-1}$) was performed with implantation of Alzet minipumps for 4 weeks (Durect Inc). All experiments involving animals were approved by the Institutional Animal Care and Use Committee at The Ohio State University.

Cardiomyocyte Isolation and Treatments

Neonatal rat ventricular cardiomyocytes were isolated as previously published.[17,18] In brief, hearts were incubated with trypsin at 4°C overnight, followed by trypsin inhibitor and collagenase incubation at 37°C for 1 hour (Worthington Biochemical). Hearts were mechanically dissociated and incubated for an additional 15 minutes, followed by resuspension in media supplemented with fetal bovine serum and preplating to remove noncardiomyocytes. Cardiomyocytes were plated on 0.1% gelatin–coated dishes in the presence of 10% serum. The following day, cells were washed twice and cultured in M199 media without serum (Corning). Hypertrophy was induced by culturing cardiomyocytes for 48 hours in the presence of 2% serum. Knockdown of METTL3 was obtained by transfection of small interfering RNA–targeting METTL3 (TriFECTa Mettl3 RNAi by Integrated DNA Technologies) or negative small interfering RNA control (TriFECTa negative control DS NC1 RNAi by Integrated DNA Technologies), and cells were analyzed 48 hours posttransfection. Overexpression of METTL3 or β-galactosidase (control) was achieved by adenoviral infection, and cells were analyzed 48 hours postinfection. Adult mouse cardiomyocytes were isolated as previously described[19] and imaged using bright field microscopy (magnification 20×) on an EVOS FL Auto II microscope (Thermo Fisher). For analysis of cardiomyocyte number, freshly isolated cardiomyocytes from 3-month-old mice were counted (before the sedimentation steps to avoid cardiomyocyte loss) with a hemocytometer. For analysis of cardiomyocyte volume, isolated cardiomyocytes from 3-month-old mice were stained in suspension with fluorescein isothiocyanate–conjugated wheat germ agglutinin (Sigma-Aldrich) and imaged with a Zeiss Confocal Microscope using a 40× objective. Z stack images were taken with a step size of 1 μm, and cardiomyocyte cell volume was calculated using the length, width, and height of the cell as adapted from Mollova et al.[20] Cardiomyocyte cell numbers in this case were determined using volume measurements in relation to heart weights of the animals from which individual cardiomyocytes were isolated; the total volume of the heart was determined from the heart weight divided by the specific gravity of muscle (1.06 g/mL).

m6A Quantification, Immunoprecipitation, RNA Sequencing, and Bioinformatics

RNA was extracted from neonatal rat cardiomyocytes using Trizol (Life Technologies). Unstimulated or hypertrophic cardiomyocyte RNA samples were subjected to m6A quantification using the m6A RNA Methylation Quantification Kit (Colorimetric) (Abcam ab185912) in biological triplicate. Adult mouse cardiomyocytes from METTL3-cKO, METTL3-TG, and littermate controls were isolated, and RNA was extracted using Trizol. m6A quantification was performed using the Abcam m6A RNA Methylation Quantification Kit described above. For genome-wide m6A profiling, 2.5 mg of total RNA was extracted from neonatal rat cardiomyocytes using Trizol and enriched for mRNAs using polyT columns. Unstimulated or hypertrophied cardiomyocyte RNA samples (in biological duplicates) were subjected to m6A immunoprecipitation as previously described.[9] In brief, mRNA was chemically fragmented and incubated with antibodies recognizing m6A-modified RNA (Synaptic Systems). Rabbit normal IgG was used as a negative control. Immunoprecipitated RNA was then submitted for RNA sequencing (University of Cincinnati sequencing and genome analysis core laboratory). Illumina reads were mapped to the rat reference genome (UCSC Rn4) using Tophat. The resulting bam files were individually analyzed for peak detection using MACS (version 1.4).[21] The peaks from all repeats were merged to build the consensus peak regions, such that the peak is included if it appears in at least 1 repeat. The reads in each consensus peak region were counted in each sample's bam file. The log2-transformed reads per kilobase million–normalized read counts were used as the peak intensity for each consensus peak region in each sample. Negative control immunoprecipitation samples were used to control for unspecific binding: peaks that appeared in the negative control as well were excluded. Peaks whose intensities were significantly different between hypertrophy and normal samples were detected by Student *t* test comparing all normal and hypertrophy replicates with a false discovery rate–adjusted *P* value <0.1. We used our own R scripts to create the analysis pipeline. This pipeline was based on the *Nature Protocol* article, "A computational pipeline for comparative ChIP-seq analyses," which contained modifications to accommodate statistical analysis of replicates.[22] Annotations of the consensus peak regions, including chromosome number, start and end location on chromosomes, gene name and identification of the peak region, and the genomic feature of the peak (5′-untranslated region, intron, exon, and 3′-untranslated region) were added according to UCSC Rn4 gene definitions. RNA sequencing data sets were submitted to the Gene Expression Omnibus database (series GSE119170). Peaks were visualized using the IGV browser.[23]

Western Blotting, Histology, Immunostaining, and mRNA Expression Analysis

Western blotting was performed from neonatal rat cardiomyocytes using standard procedures. Antibodies used were METTL3 (Bethyl Laboratories), MAP3K6 (Novus Biologicals), MAP4K5 (Thermo Scientific Pierce), MAPK14 (Cell Signaling Technology), and GAPDH (Fitzgerald Industries). Masson trichrome staining was performed from histological sections generated from paraffin-embedded hearts. Immunostaining was performed using α-actinin antibodies (Sigma-Aldrich), and cell area was quantified using CellProfiler following published methods.[24] Detection of the cell membrane was performed using fluorescein isothiocyanate–conjugated wheat germ agglutinin (Sigma-Aldrich). The cross-sectional area was measured using ImageJ. RNA was extracted from neonatal rat cardiomyocytes or mouse hearts using Trizol, and reverse transcription was performed using the High Capacity cDNA Reverse Transcription kit (Applied Biosystems). Selected genes and m6A peaks were analyzed by real-time polymerase chain reaction using SYBR green (Applied Biosystems). Quantified mRNA expression was normalized to Rpl7 (ribosomal protein L7) and expressed relative to controls.

Statistics

All results are presented as mean±SEM. Statistical analysis was performed with an unpaired 2-tailed *t* test (for 2 groups) and 1-way ANOVA with Bonferroni correction (for groups of ≥3). *P* values <0.05 were considered significant.

RESULTS

m6A Is a Dynamic Modification in Cardiomyocytes

To determine the mRNAs that are modified by m6A methylation in cardiomyocytes, we performed m6A sequencing on cultured rat neonatal cardiomyocytes. Purified mRNAs were fragmented to allow for analysis of the specific location of m6A peaks, pulled down using a specific antibody recognizing m6A-modified RNA, and processed for sequencing (m6A sequencing, meRIP-seq). Using this strategy, we identified 3922 m6A peaks that showed a general distribution throughout the coding region of genes (Figure 1A and Table II in the online-only Data Supplement). We also detected relative enrichment on the untranslated regions, consistent with previous reports[9] (Figure 1A and Table II in the online-only Data Supplement). To assess a possible role for m6A modifications on mRNA in the development of cardiomyocyte hypertrophy, we performed an independent m6A quantification experiment where we assessed if the overall percentage of m6A in RNA changes during cardiomyocyte hypertrophy. We used serum as a prohypertrophic stimulus and isolated RNA from neonatal rat cardiomyocytes. Using an antibody-mediated capture of m6A followed by colorimetric analysis, we determined that the percentage of m6A RNA modification increases substantially in response to a hypertrophic stimulus (Figure 1B). To define the specific mRNA sequences that were dynamically affected by m6A modification in response to a hypertrophic stimulus, we performed m6A sequencing of m6A-modified mRNA from hypertrophic cardiomyocytes in comparison with unstimulated conditions. Our analysis revealed differential m6A methylation during hypertrophy on 713 cardiomyocyte mRNAs (Table III in the online-only Data Supplement). It is interesting to note that we found that, in hypertrophic cardiomyocytes, m6A changes are not randomly distributed throughout the genome, but are specifically increased in select classes of mRNAs (Figure 1C). Within these specific functional categories, m6A peaks in mRNAs encoding for protein kinases and modifiers were the most significantly enriched during hypertrophy (Figure 1C). Representative m6A peaks in the ryanodine receptor (Ryr2) and mitogen-activated protein kinase kinase kinase 6 (Map3k6) 3′-untranslated regions are shown as examples of m6A-methylated mRNA that showed either no change with hypertrophy (Ryr2) or increased levels of m6A with hypertrophy (Map3k6) (Figure 1D and 1E). To validate the results of m6A sequencing and quantify the extent of enhanced methylation in response to a hypertrophic stimulus, we performed m6A immunoprecipitation followed by real-time polymerase chain reaction using gene-specific primers flanking the identified m6A peaks from RNA sequencing (Table 1). We assessed increased m6A levels following hypertrophic stimulus in 16 genes from the functional category of protein-modifying enzymes that showed increased m6A levels following hypertrophic stimulus in our genome-wide analysis, and identified 15 to be significantly enriched for m6A. These results clearly show that m6A modifications on mRNA are enhanced on specific classes of proteins in response to a hypertrophic stimulus.

METTL3 Drives Cardiomyocyte Hypertrophy In Vitro and In Vivo

To determine whether enhancing m6A modification on mRNA was sufficient to cause cardiomyocyte hypertrophy, we tested how overexpression of the m6A-catalyzing enzyme METTL3 affects cardiomyocytes. Specifically, we generated an adenoviral vector to increase METTL3 expression in cardiomyocytes. We infected cardiomyocytes under unstimulated conditions, and used adenovirus encoding for β-galactosidase as a negative control. We first verified that METTL3 was indeed expressed at higher levels (Figure 2A). We also tested if METTL3 overexpression affected protein levels of m6A-methylated mitogen-activated protein kinases and found that METTL3 enhanced the levels of MAP3K6, MAP4K5, and MAPK14 in cardiomyocytes (Figure 2A and 2B). It is remarkable that upregulation

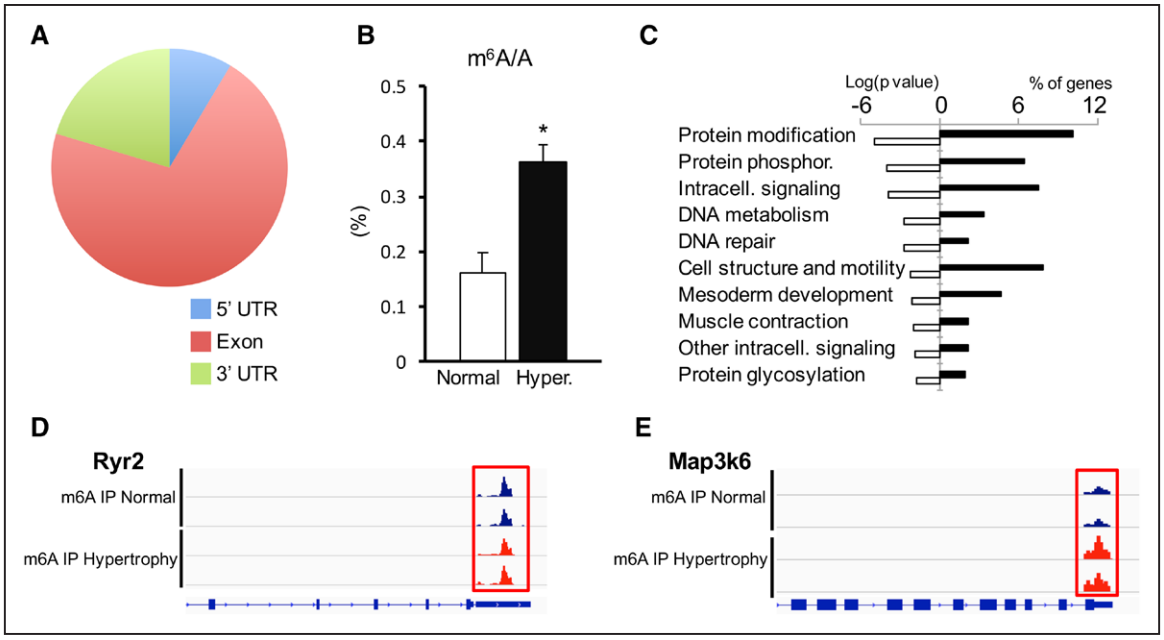

Figure 1. m6A is a dynamic modification in cardiomyocytes.
A, Distribution of m6A peaks throughout mRNAs. **B**, Percentage of m6A-methylated RNA in relation to unmodified adenosine as quantified using an antibody-mediated m6A capture assay in unstimulated (Normal) and hypertrophic (Hyper.) neonatal rat cardiomyocytes (n=3 each). **C**, PANTHER analysis of enriched functional gene categories showing differential m6A peaks during hypertrophy. **D** and **E**, Visualization of representative m6A peaks under unstimulated or hypertrophic conditions from the indicated mRNAs using Integrative Genomics Viewer. *$P \leq 0.05$ versus normal. Intracell. indicates intracellular; IP, immunoprecipitation; Map3k6, mitogen-activated protein kinase kinase kinase 6; m6A, N^6-Methyladenosine; PANTHER, Protein Analysis through Evolutionary Relationships; phosphor., phosphorylation; Ryr2, ryanodine receptor; and UTR, untranslated region.

of METTL3 caused a significant increase in cardiomyocyte size, indicating that METTL3 expression is sufficient to cause cardiomyocyte hypertrophy (Figure 2C and 2D). We also validated that the m6A mRNA targets we identified using isolated neonatal rat cardiomyocytes were also relevant in the adult heart. To this end, we performed m6A immunoprecipitations from neonatal and adult mouse heart RNA followed by real-time polymerase chain reaction. With the exception of STE20-like protein kinase 4 (Mst4), we found that all m6A peaks identified in the isolated neonatal cardiomyocyte screen were also present in the adult heart (Table 2). This experiment also revealed that m6A methylation of the tested mRNAs was, in many cases, higher in adult hearts than in the neonatal state, in agreement with overall higher m6A levels in adult hearts (Table 2 and Figure IA in the online-only Data Supplement). These findings suggest a role for m6A mRNA methylation in adult cardiac homeostasis.

To further verify a role for m6A in regulating cardiomyocyte homeostasis and hypertrophy in the adult heart, we generated a METTL3-overexpressing (METTL3-TG or M3-TG) mouse line by cross-breeding a transgenic αMHC promoter–driven tetO responder with the αMHC–tetracycline transactivator driver to impart gene expression specifically in cardiomyocytes (Figure 2E and 2F). METTL3-overexpressing mice showed a significant increase in m6A levels in cardiomyocyte RNA and dose-dependent cardiac hypertrophic growth at 3 months of age (Figure 2G and 2H). The lowest expressing line was then further characterized to follow the progression of cardiac remodeling over time. We found that this line

Table 1. m6A Modification on Specific mRNAs in Response to Hypertrophy

Gene	Normal	Hypertrophy	*P* Value
Dapk1	1.04±0.11	9.87±0.77	<0.001
Dclk2	1.01±0.12	36.59±11.76	0.039
Grk4	1.82±1.06	25.49±5.98	0.018
Ikbkap	1.01±0.13	5.23±0.82	0.007
Ikbkb	1.08±0.27	9.14±0.85	0.001
Krs1	1.17±0.47	9.60±2.73	0.038
Map3k14	1.03±0.21	16.30±3.59	0.013
Map3k6	1.03±0.19	15.85±1.89	0.001
Map4k5	0.97±0.27	5.77±2.81	0.164
Mapk14	1.13±0.37	8.19±1.52	0.011
Mst4	1.01±0.13	18.75±2.98	0.004
Nuak2	1.00±0.07	8.16±2.16	0.030
Rps6ka2	1.04±0.20	8.32±1.79	0.015
Rps6ka4	1.04±0.20	8.32±1.79	0.015
Rps6ka5	1.03±0.19	16.12±1.92	0.001
Sgk1	1.07±0.26	13.05±2.56	0.010

m6A immunoprecipitation was performed followed by qPCR using primers designed around preidentified m6A peaks. The qPCR data were corrected to overall gene expression level under the same conditions (normal versus hypertrophy). Data represented are average±SEM from 3 biological replicates each. m6A indicates N^6-Methyladenosine; and qPCR, quantitative polymerase chain reaction.

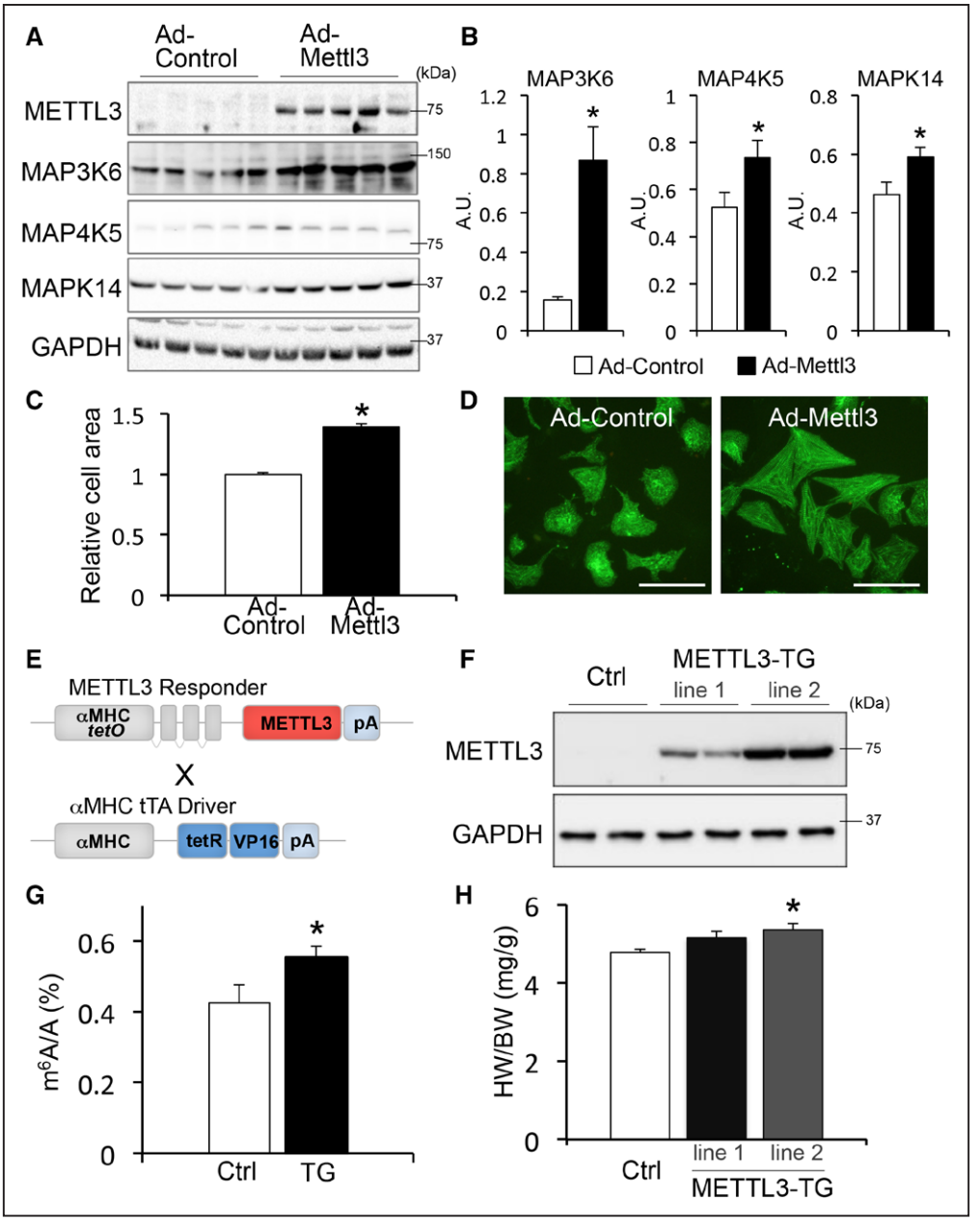

Figure 2. Generation and characterization of METTL3 overexpression models.
A, Western blot from cardiomyocytes overexpressing β-galactosidase (Ad-Control) or METTL3 (Ad-Mettl3) using antibodies against the indicated proteins and GAPDH loading control. **B,** Densitometry quantification of the expression for the indicated proteins relative to GAPDH control. **C**, Quantification of cardiomyocyte cell area based on pixel size from cardiomyocytes overexpressing β-galactosidase control or METTL3 (n=3 each). **D**, Representative images of cardiomyocytes from the indicated treatments stained for α-actinin (green). Scale bar=20 μm. **E,** Schematic of cardiomyocyte-specific METTL3 gain-of-function mouse model. **F,** Western blot from cardiac extracts from control (Ctrl) or METTL3 transgenic (TG) line 1 and 2. GAPDH was used as loading control. **G**, percentage of m6A-methylated RNA relative to unmodified adenosine as quantified using an antibody-mediated m6A capture assay in isolated cardiomyocytes from control mice and METTL3 TG line 1 mice (n=3 each). **H**, Gravimetric analysis of heart weight normalized to body weight (HW/BW) in the indicated genotypes at 3 months of age (n≥6 each). **P*<0.05 versus control. A.U. indicates arbitrary units; m6A, N^6-Methyladenosine; and METTL3, methyltransferase-like 3.

expresses, on average, 19-fold higher levels of METTL3 in the heart than control mice (Figure IB and IC in the online-only Data Supplement).

By 8 months of age, METTL3-overexpressing mice exhibit cardiac hypertrophy, as demonstrated by increased heart weight to body weight ratios (Figure 3A). Cardiac hypertrophic growth was accompanied by a larger cardiomyocyte cross-sectional area (Figure 3B and 3C). Analysis of isolated adult cardiomyocytes revealed physiological growth of cardiomyocytes in both width and length, resulting in a preserved length-to-width ratio (Figure 3D and 3E). However, despite the structural changes METTL3-TG hearts undergo, no histopathologic changes were observed in these mice (Figure 3F). It is important to note that cardiac function, as measured by echocardiographic analysis of the percentage frac-

Table 2. m6A Modification on Specific mRNAs in the Neonatal and Adult Heart

Gene	Neonatal	Adult	*P* Value
Dapk1	1.01±0.08	2.00±0.40	0.053
Dclk2	1.83±0.78	1.07±0.55	0.459
Grk4	1.09±0.25	0.78±0.13	0.273
Ikbkap	1.10±0.30	0.90±0.27	0.642
Ikbkb	1.16±0.34	1.25±0.38	0.863
Krs1	1.03±0.16	1.67±0.37	0.162
Map3k14	1.06±0.24	3.11±0.82	0.075
Map3k6	1.11±0.21	3.73±0.48	0.0005
Map4k5	1.18±0.34	0.95±0.26	0.602
Mapk14	1.10±0.26	1.89±0.17	0.043
Mst4	N/A	N/A	N/A
Nuak2	1.00±0.01	3.92±0.72	0.018
Rps6ka2	1.12±0.29	2.17±0.40	0.075
Rps6ka4	1.09±0.32	4.69±0.40	0.002
Rps6ka5	1.03±0.14	3.75±0.76	0.012
Sgk1	1.03±0.13	2.02±0.46	0.086

m6A immunoprecipitation was performed followed by qPCR using primers designed around preidentified m6A peaks. The qPCR data were corrected to overall gene expression level under the same conditions (neonatal versus adult). Data represented are average±SEM from 4 biological replicates each. m6A indicates N^6-Methyladenosine; N/A, not available; and qPCR, quantitative polymerase chain reaction.

tional shortening, was preserved (Figure 3G). To further confirm the adaptive nature of the cardiac remodeling observed in METTL3-TG mice and ensure that it does not accelerate dysfunction during stress, we performed pressure overload stimulation on 3-month-old METTL3-TG and control mice through transverse aortic constriction. We found that increased expression of METTL3 is not detrimental post stress (Figure 3H). Also, the hypertrophic response to transverse aortic constriction was not exacerbated by METTL3 upregulation at the organ level or in terms of cardiomyocyte cross-sectional area (Figure 3I through 3K). Therefore, enhancing m6A modification of mRNA through cardiomyocyte-specific METTL3 overexpression induces compensated hypertrophic remodeling of the heart without inducing cardiac functional deficits either at baseline or under cardiac stress.

METTL3 Inhibition Prevents the Development of Cardiomyocyte Hypertrophy in Vitro

To determine if m6A methylation plays a primary role in the development of cardiac hypertrophy, we inhibited expression of the m6A-catalyzing enzyme METTL3 in isolated neonatal rat cardiomyocytes. We observed a significant knockdown of METTL3 by delivery of METTL3-targeting small interfering RNA (Figure 4A). In the absence of hypertrophic stimuli, we did not observe any changes in cardiomyocyte size. However, on stimulation of cardiomyocyte hypertrophy through the addition of serum, we noticed a normal hypertrophic response in control small interfering RNA–treated cardiomyocytes, but a complete block of hypertrophy when METTL3 was knocked down (Figure 4B and 4C).

Cardiomyocyte-Specific METTL3 Knockout Induces Cardiac Structural and Functional Changes With Aging and Stress

To determine the necessity of METTL3 and m6A in the heart, we generated a cardiomyocyte-specific METTL3 knockout (METTL3-cKO) mouse line using a typical (β-MHC promoter driven) cardiomyocyte-specific cre-loxP system (Figure 5A and 5B). Consistent with their METTL3 knockout status, METTL3-cKO mice have significantly decreased m6A levels in comparison with their littermate controls (Figure 5C). Three-month-old METTL3-cKO animals do not show cardiac morphological or functional changes, indicating that METTL3 knockout does not impair cardiac development (Figure 5D through 5H). Specifically, no histopathologic and hypertrophic changes were observed (Figure 5D and 5E). Also, cardiac function was unaffected as measured by echocardiographic analysis of the percentage fractional shortening (Figure 5F). To confirm the absence of remodeling at the cellular level, we then measured cardiomyocyte cross-sectional area and observed no changes in METTL3-cKO mice (Figure 5G and 5H). To further exclude developmental defects in METTL3-cKO mice, we assessed postnatal proliferative and hypertrophic growth (Figure II in the online-only Data Supplement). Expression analysis of proliferation markers revealed no abnormalities in METTL3-cKO hearts (Figure IIA through IIC in the online-only Data Supplement). Similarly, markers of hypertrophy and the postnatal switch between β- and α-MHCs (Myh7 and Myh6, respectively) were also unaffected (Figure IID through IIF in the online-only Data Supplement). Considering that, within the first week of life, murine cardiomyocytes lose their ability to grow by hyperplasia and instead activate a postnatal hypertrophic program, we tested cardiomyocyte cross-sectional area in day 7 hearts from METTL3-cKO and control mice. This analysis revealed that postnatal growth is unaffected in the absence of METTL3 (Figure IIG and IIH in the online-only Data Supplement). Consequently, cardiomyocyte numbers and cell volumes in 3-month-old METTL3-cKO and control mice were also unchanged (Figure II I through IIK in the online-only Data Supplement). Overall, these results suggest that METTL3 is dispensable for postnatal heart development.

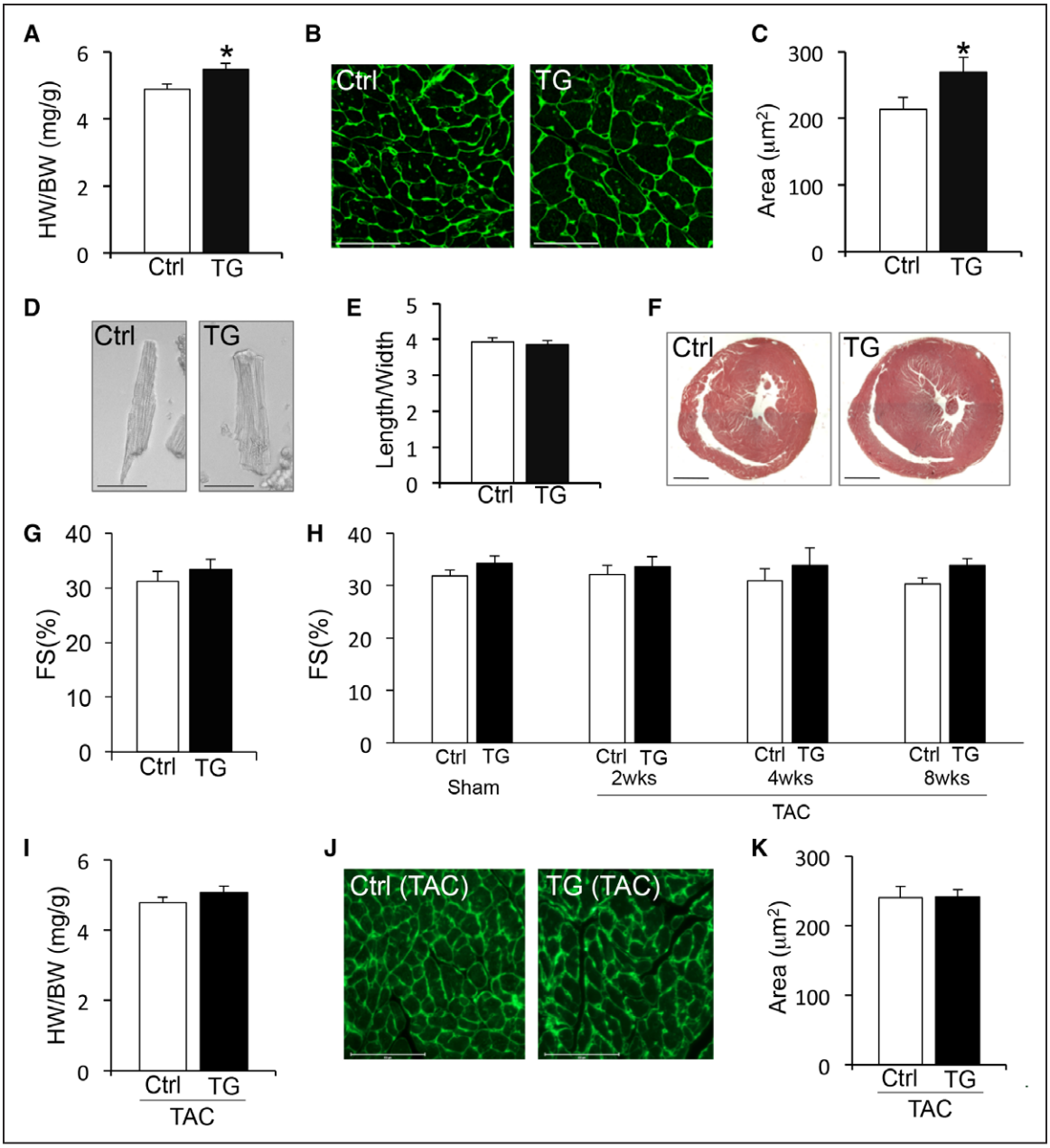

Figure 3. METTL3 drives compensated hypertrophy in vivo.
A, Heart weight to body weight ratios (HW/BW) in 8-month-old METTL3-TG animals or littermate controls (n≥7 each group). **B** and **C**, Wheat germ agglutinin (green)–stained cardiac cross-sections of 8-month-old METTL3-TG or littermate control mice with quantification of cardiomyocyte cross-sectional area using ImageJ software. Scale bar=50 μm (n≥100 cells/animal, n=6 mice each). **D**, Representative images of isolated cardiomyocytes from 8-month-old hearts from the indicated genotypes. Scale bar=50 μm. **E**, Length/width ratios of isolated cardiomyocytes from 8-month-old control and TG mice (n≥100 cells/animal; n=3 mice each). **F**, Representative images of Masson trichrome staining of cardiac cross-sections of 8-month-old METTL3-TG or littermate control mice. Scale bar=1 mm. **G**, Echocardiographic quantification of percentage fractional shortening (FS) for 8-month-old METTL3-TG animals or littermate controls (n=12 each). **H**, Echocardiographic quantification of percentage fractional shortening for Sham or TAC-operated METTL3-TG animals or littermate controls (n≥5 each). **I**, HW/BW in TAC-operated METTL3-TG animals or littermate controls (n≥5 each group). **J** and **K**, Wheat germ agglutinin (green)–stained cardiac cross-sections of TAC-operated METTL3-TG or littermate control mice with quantification of cardiomyocyte cross-sectional area using ImageJ software. Scale bar=100 μm (n≥100 cells/animal, n=5 mice each). *P≤0.05 versus Ctrl. Ctrl indicates control; METTL3, methyltransferase-like 3; TAC, transverse aortic constriction; and TG, transgenic.

However, when METTL3-cKO animals are aged to 8 months, they begin to show cardiac abnormalities consistent with a progression toward heart failure (Figure 6). Cardiomyocyte cross-sectional area was significantly reduced in 8-month-old METTL3-cKO mice (Figure 6A and 6B). It is interesting that these changes were not accompanied by overall heart weight alterations (Figure 6C). To further understand these results, we isolated adult cardiomyocytes and found eccentric cardiomyocyte remodeling in the absence of METTL3 (Figure 6D through 6F). Indeed, cardiomyocytes from METTL3-cKO hearts were elongated and showed an

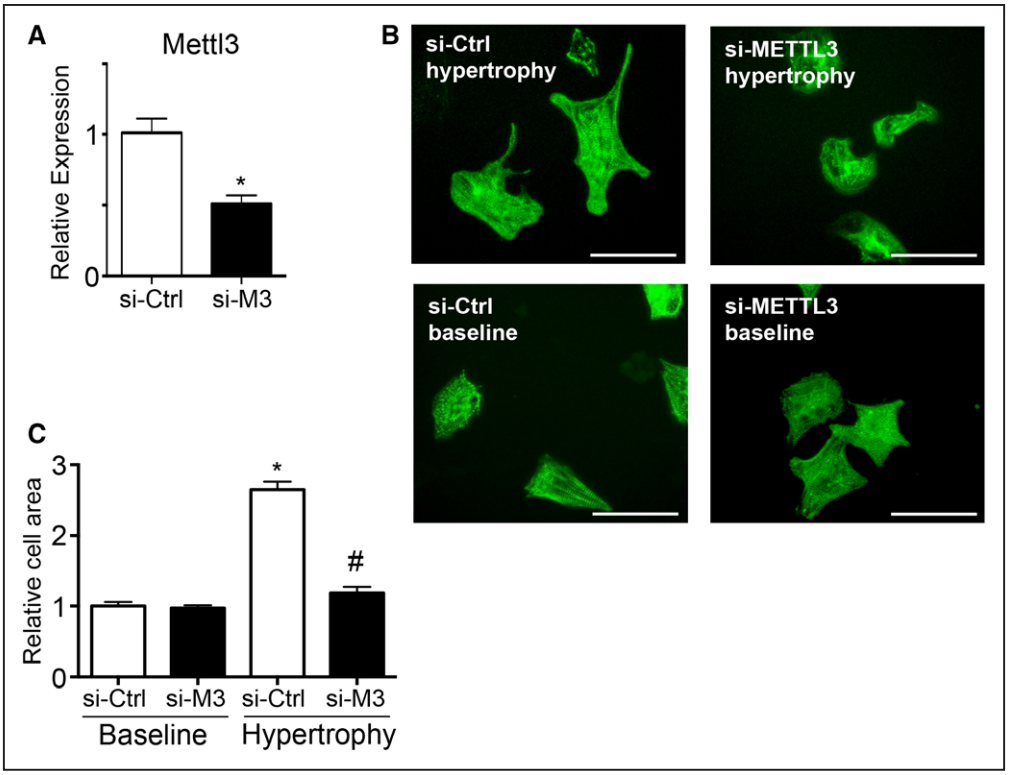

Figure 4. METTL3 inhibition prevents the development of cardiomyocyte hypertrophy.
A, qPCR analysis for METTL3 expression in response to Ctrl or METTL3 siRNA-mediated knockdown (n=3 each). **B**, Representative images of cardiomyocytes treated with control siRNA (si-Ctrl) or siRNA targeting METTL3 (si-M3) stained for α-actinin (green). Scale bar=20 μm. **C**, Quantification of cardiomyocyte cell area (n≥50 cells/well, n=3 independent experiments/treatment). **P*<0.05 versus baseline; #*P*<0.05 versus si-Ctrl hypertrophy. Ctrl indicates control; METTL3, methyltransferase-like 3; siRNA, small interfering RNA; and qPCR, quantitative polymerase chain reaction.

overall increase in their length-to-width ratio (Figure 6F). Consistent with maladaptive eccentric cardiomyocyte remodeling, cardiac knockout of METTL3 caused a significant increase in left ventricular chamber dimensions and ventricular dilation (Figure 6G through 6I). The structural changes we observed in METTL3-cKO cardiomyocytes were also associated with a decrease in overall cardiac function as measured by echocardiography (Figure 6J).

To test if METTL3 is necessary for adaptation to stress, we then subjected 3-month-old METTL3-cKO and control mice to pressure overload stimulation (or transverse aortic constriction). We found that the absence of METTL3 accelerates heart failure progression and leads to reduced cardiomyocyte cross-sectional area (Figure 7A through 7C). These data suggest that METTL3 is critical for adaptive cardiac remodeling after injury. To further test if maladaptive cardiomyocyte remodeling occurs before dysfunction and could indeed be a pathological driver of cardiomyopathy, we applied a milder stress through the infusion of angiotensin and phenylephrine for 4 weeks. In this condition in which cardiac function was still intact, we observed reduction in the cross-sectional area of stressed cardiomyocytes lacking METTL3 (Figure 7D through 7F). This result indicates a direct role for METTL3 in controlling cardiomyocyte geometry and adaptation to stress.

Altogether, our data demonstrate a critical role for METTL3 and m6A modifications of mRNA for the maintenance of cardiac homeostasis, function, and stress responses.

DISCUSSION

The control of protein synthesis is achieved by complex and still poorly defined mechanisms that regulate the posttranscriptional processing of mRNAs. Understanding how specific classes of functionally related mRNAs are coregulated in the heart is crucial to elucidate the molecular mechanisms controlling the characteristic increase in cardiac mass that defines cardiac hypertrophy within myocytes. Here, we discovered METTL3 as a critical RNA-modifying protein that drives cardiomyocyte hypertrophy by catalyzing methylation of m6A on specific subsets of mRNAs. Our genome-wide m6A-sequencing analysis in cardiomyocytes represents the first report demonstrating the occurrence of m6A in cardiac cells, the dynamic changes occurring in hypertrophic conditions, and the specific mRNA targets of this modification. An interesting result from our analysis was the discovery of protein kinases as the most affected cat-

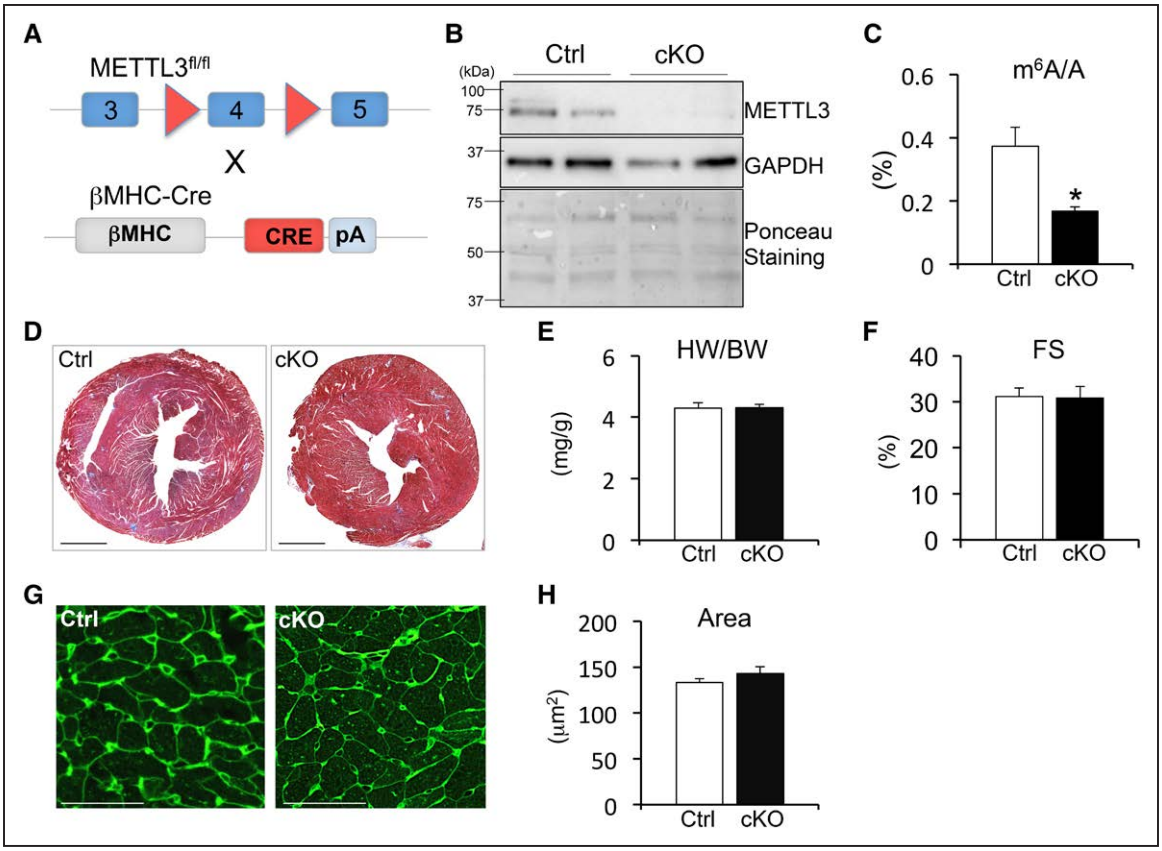

Figure 5. Generation and characterization of METTL3 cardiac-restricted knockout mice.
A, Schematic of METTL3 loss-of-function mouse model. **B**, Western blot for METTL3 from cardiac extracts from control (Ctrl) or cardiomyocyte-specific METTL3 knockout mice (cKO). GAPDH and Ponceau staining were used as loading control. **C**, percentage of m6A-methylated RNA relative to unmodified adenosine as quantified using an antibody-mediated m6A capture assay in isolated cardiomyocytes from control and METTL3-cKO mice (n=3 each). **D,** Representative Masson trichrome–stained cardiac cross-sections from 3-month-old METTL3-cKO mice and controls. Scale bar=1 mm. **E,** Quantification of heart weight to body weight ratio (HW/BW) for 3-month-old METTL3-cKO or control mice (n=5 each). **F**, Echocardiographic quantification of percentage fractional shortening (FS) for 3-month-old METTL3-cKO or control mice (n=12 each). **G** and **H**, Wheat germ agglutinin (green)–stained cardiac cross-sections of 3-month-old METTL3-cKO or control mice with quantification of cardiomyocyte cross-sectional area. Scale bar=50 μm (n≥100 cells/animal, n≥4 mice each). **P*≤0.05 versus Ctrl. m6A indicates *N*6-Methyladenosine; and METTL3, methyltransferase-like 3.

egory of genes dynamically controlled by the METTL3-m6A pathway during hypertrophy. Indeed, many studies have recognized the importance of kinase-regulated signaling pathways for cardiomyocyte hypertrophic growth, and mitogen-activated protein kinases specifically have well-established roles in hypertrophy.[25] In addition, we also found hypertrophy-dependent methylation on mRNAs encoding for kinases converging on the nuclear factor kB, which has been shown to cooperate not only with mitogen-activated protein kinases, but also with nuclear factor of activated T cells in regulating cardiac hypertrophy.[26] Last, our m6A profile revealed dynamic methylation in mRNAs encoding for members of the ribosomal S6 family of kinases. Ribosomal S6 kinases are downstream effectors of the extracellular regulated kinase branch of mitogen-activated protein kinases and have established roles in adaptive cardiac growth through the regulation of mammalian target of rapamycin–dependent protein synthesis.[27,28] Considering the complexity and intersection of multiple signaling mechanisms driving cardiac hypertrophy, the discovery of METTL3 as a master controller of large subsets of signaling molecules through posttranscriptional regulation of mRNA processing might further explain how stress responses are coordinated at a posttranscriptional level in cardiomyocytes. Our findings open intriguing new possibilities for controlling cardiac remodeling and pathological stress responses in the heart.

It is striking to observe how m6A levels increase in specific functional clusters of mRNAs in response to hypertrophic growth signals in cardiomyocytes. Although the origin of this specificity is currently unknown, the fact that increased expression of METTL3 is sufficient to cause hypertrophy might indicate that the activity of this enzyme could be a limiting factor under homeostatic conditions. In addition, it is important to consider that specific demethylases might act with different specificity, and their activity could also be controlled by hypertrophic signals in cardiomyocytes. Indeed, the m6A epigenetic mark has been shown to be reversible.[8] The protein that removes the methyl group m6A was identified as fat mass and obe-

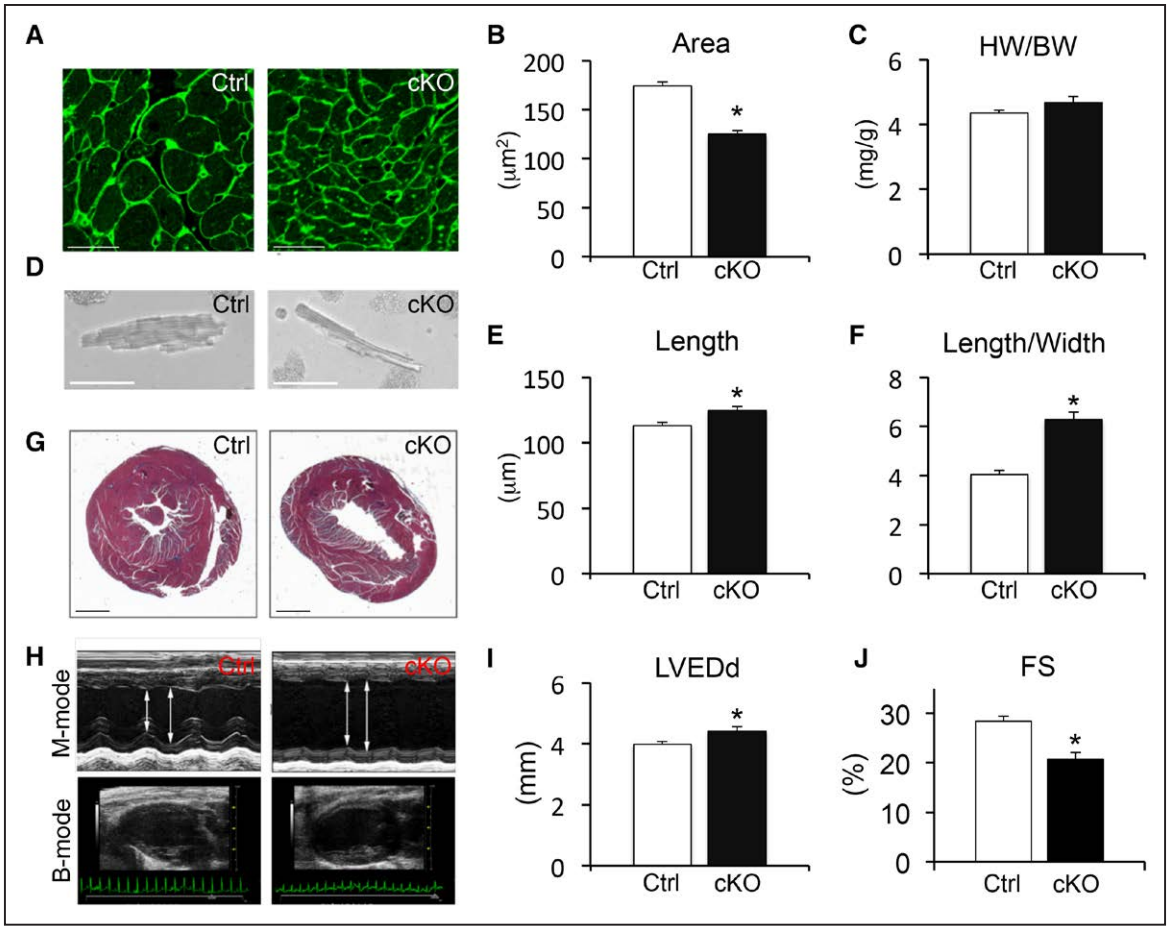

Figure 6. METTL3 loss-of-function causes maladaptive cardiomyocyte remodeling and cardiac dysfunction with aging.
A and **B**, Wheat germ agglutinin–stained cardiac cross-sections of 8-month-old METTL3-cKO or control mice with quantification of cardiomyocyte cross-sectional area. Scale bar=50 μm (n≥100 cells/animal, n≥5 mice each). **C**, Quantification of heart weight to body weight ratio (HW/BW) for 8-month-old METTL3-cKO or control mice (n≥13 each). **D** and **F**, Representative bright field image of isolated cardiomyocytes from the indicated genotypes at 8 months of age (**D**) and measurements of length (**E**) and length/width ratios (**F**) (n≥100 cells/animal; n=3 animals each). Scale bar=50 μm. **G**, Representative Masson trichrome–stained cardiac cross-sections from 8-month-old METTL3-cKO mice and control mice. Scale bar=1 mm. **H** through **J**, Representative images of short-axis (M-mode) and long-axis (B-mode) echocardiographic analysis (**H**), and echocardiographic quantification of left ventricular chamber end-diastolic dimensions (LVEDd) (**I**) and percentage fractional shortening (FS) (**J**) in 8-month-old METTL3-cKO and control mice (n=18 each). *P≤0.05 versus Ctrl. cKO indicates cardiomyocyte-specific METTL3 knockout mice; Ctrl, control; and METTL3, methyltransferase-like 3.

sity associated protein (FTO), a member of the alkylation repair homologs (ALKBH) family.[29] Furthermore, METTL3 acts in a complex composed of methyltransferase-like 14 (METTL14) and additional regulatory subunits, Wilms tumor 1–associating protein (WTAP) and KIAA1429.[30,31] It is becoming clear that, although the METTL3-containing protein complex is ubiquitously responsible for the deposition of the m6A epigenetic mRNA mark, different ALKBH proteins have acquired some level of tissue specificity, and the relative contribution of each specific member in demethylating m6A from RNA is still unclear.[32] In addition to m6A writers and erasers, m6A recognition factors (or readers) have also been discovered and are members of the YT521-B homology domain family.[33] Readers, together with writers and erasers, contribute to the overall regulation of m6A-mRNA biology.

The m6A modification is part of the larger field of RNA epigenetics, which is a growing field that is only beginning to be explored in the heart.[34] Similar to the deposition of epigenetic marks on DNA, methylation of mRNAs can impact gene expressivity and define the fate of subgroups of mRNAs. This is especially important for stress-response pathways that need to rapidly react to environmental challenges. Indeed, transcription is time-consuming, and cells have devised methods to preserve pools of mRNAs that can be readily and dynamically available for translation.[35] Our study shows the importance of m6A mRNA modification as a dynamic epigenetic mark that cardiomyocytes use to respond to hypertrophic stimuli. It is also interesting to note that enhancing the METTL3-m6A pathway was sufficient to induce cardiomyocyte hypertrophy in the absence of additional stimuli, and that inhibition of METTL3 was sufficient to block hypertrophy in vitro. It is intriguing that our data on newly generated gain- and loss-of-function mouse models revealed that modulation of METTL3 is sufficient to govern cardio-

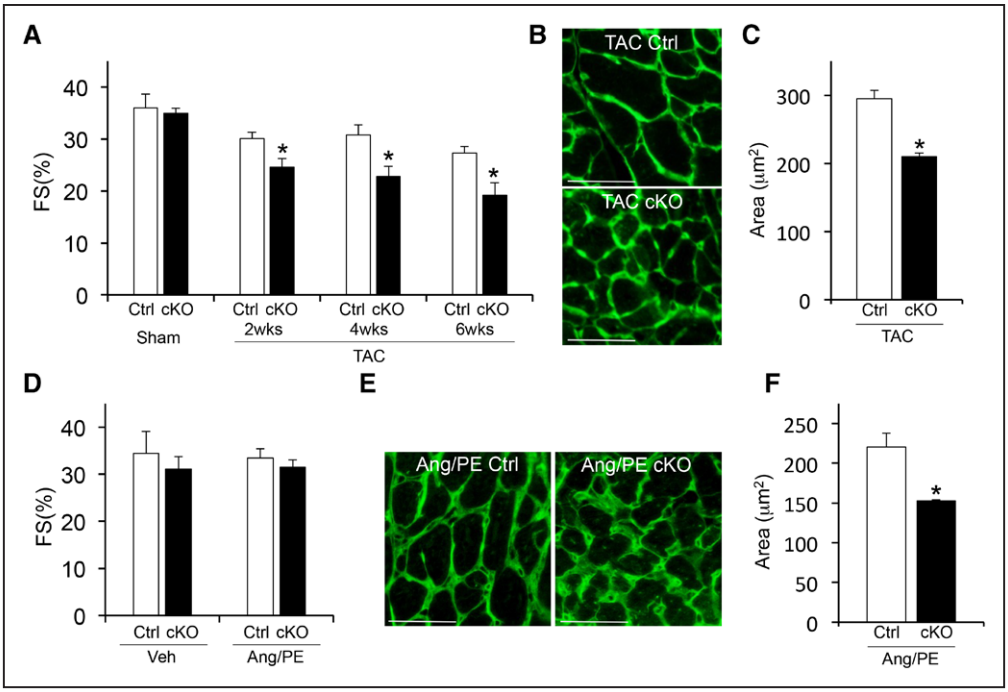

Figure 7. METTL3 loss-of-function causes maladaptive cardiomyocyte remodeling and cardiac dysfunction poststress.
A, Echocardiographic quantification of percentage fractional shortening (FS) in 3-month-old METTL3-cKO and control mice subjected to sham or TAC surgery for the indicated times (n=8 each). **B** and **C**, Wheat germ agglutinin–stained cardiac cross-sections of METTL3-cKO or control mice subjected to 6 weeks of TAC with quantification of cardiomyocyte cross-sectional area. Scale bar=50 μm (n≥100 cells/animal, n=7 mice each). **D**, Echocardiographic quantification of percentage FS in 3-month-old METTL3-cKO and control mice subjected to vehicle (Veh) or angiotensin/phenylephrine infusion (Ang/PE) for 4 weeks (n=5 each). **E** and **F**, Wheat germ agglutinin–stained cardiac cross-sections of METTL3-cKO or control mice subjected to 4 weeks of vehicle orAng/PE with quantification of cardiomyocyte cross-sectional area. Scale bar=50 μm (n≥100 cells/animal, n≥3 mice each). **P*≤0.05 versus Ctrl. cKO indicates cardiomyocyte-specific METTL3 knockout mice; Ctrl, control; METTL3, methyltransferase-like 3; and TAC, transverse aortic constriction.

myocyte geometry and function with aging and during 2 forms of cardiac stress, pointing to the METTL3-m6A pathway as a novel critical mediator of cardiac homeostasis.

Preservation of physiological cardiomyocyte geometry is critical for cardiac function. Cardiomyocytes initially grow in a concentric manner following hemodynamic stress, but elongate eccentrically during cardiomyopathic dilation and heart failure.[1,36] Growth of cardiomyocytes is also present during physiological stimuli of the heart, such as exercise, helping maintain cardiac output in the face of increased afterload.[1,36] We found that perturbing the level of METTL3 and m6A is sufficient to induce spontaneous cardiomyocyte remodeling, because increased m6A led to adaptive growth, whereas decreased m6A induced eccentric and detrimental cardiomyocyte geometry. Before our study, members of the Mapk family of kinases were one of the few examples of such a spontaneous regulation of cardiomyocyte shape.[36] Our findings are in line with these previous results, because we found that m6A modification is specifically occurring on protein kinase mRNAs, including several members of the Mapk signaling cascade. This indicates that METTL3 is able to control a gene expression program in cardiomyocytes that is responsible for the regulation of cardiac remodeling and function, suggesting a key role for METTL3 in the heart and a potential therapeutic benefit of targeting this pathway for pathological cardiac remodeling.

ARTICLE INFORMATION

Received May 25, 2018; accepted October 11, 2018.

The online-only Data Supplement is available with this article at https://www.ahajournals.org/doi/suppl/10.1161/circulationaha.118.036146.

Correspondence

Federica Accornero, PhD, Davis Heart and Lung Research Institute, Department of Physiology and Cell Biology, The Ohio State University, 473 W 12th Ave, Columbus, OH 43210. Email Federica.Accornero@osumc.edu

Affiliations

Department of Physiology and Cell Biology (L.E.D., F.A.), Department of Biomedical Engineering (X.X., T.J.H.), Dorothy M. Davis Heart and Lung Research Institute, The Ohio State University, Columbus. Department of Molecular Genetics, Weizmann Institute of Science, Rehovot, Israel (L.L., J.H.H.). Division of Biostatistics and Bioinformatics, Department of Environmental Health, University of Cincinnati, OH (J.C., M.M.). Cardiovascular Division, Lillehei Heart Institute and Stem Cell Institute, University of Minnesota, Minneapolis (J.H.v.B.).

Sources of Funding

This work was supported by grants from the National Institutes of Health (HL112852 and HL130072 to Dr van Berlo, HL121284 and HL136951 to Dr Accornero, and HL134616 to L.E. Dorn); the American Heart Association (AHA 17IRG33460198 to Dr Accornero); The Israel Science Foundation (355/17 and 107/14), the Flight Attendant Medical Research Council, the New York Stem

Cell Foundation, and the European Research Council Consolidator Grant Cell-Naivety (to Dr Hanna); and The United States-Israel Binational Science Foundation (2017094 to Drs Accornero and Hanna).

Disclosures

None.

REFERENCES

1. Kehat I, Molkentin JD. Molecular pathways underlying cardiac remodeling during pathophysiological stimulation. *Circulation*. 2010;122:2727–2735. doi: 10.1161/CIRCULATIONAHA.110.942268
2. Hannan RD, Jenkins A, Jenkins AK, Brandenburger Y. Cardiac hypertrophy: a matter of translation. *Clin Exp Pharmacol Physiol*. 2003;30:517–527.
3. Akazawa H, Komuro I. Roles of cardiac transcription factors in cardiac hypertrophy. *Circ Res*. 2003;92:1079–1088. doi: 10.1161/01.RES.0000072977.86706.23
4. Maier T, Güell M, Serrano L. Correlation of mRNA and protein in complex biological samples. *FEBS Lett*. 2009;583:3966–3973. doi: 10.1016/j.febslet.2009.10.036
5. Gao C, Ren S, Lee JH, Qiu J, Chapski DJ, Rau CD, Zhou Y, Abdellatif M, Nakano A, Vondriska TM, Xiao X, Fu XD, Chen JN, Wang Y. RBFox1-mediated RNA splicing regulates cardiac hypertrophy and heart failure. *J Clin Invest*. 2016;126:195–206. doi: 10.1172/JCI84015
6. Jonas S, Izaurralde E. Towards a molecular understanding of microRNA-mediated gene silencing. *Nat Rev Genet*. 2015;16:421–433. doi: 10.1038/nrg3965
7. Guo W, Schafer S, Greaser ML, Radke MH, Liss M, Govindarajan T, Maatz H, Schulz H, Li S, Parrish AM, Dauksaite V, Vakeel P, Klaassen S, Gerull B, Thierfelder L, Regitz-Zagrosek V, Hacker TA, Saupe KW, Dec GW, Ellinor PT, MacRae CA, Spallek B, Fischer R, Perrot A, Özcelik C, Saar K, Hubner N, Gotthardt M. RBM20, a gene for hereditary cardiomyopathy, regulates titin splicing. *Nat Med*. 2012;18:766–773. doi: 10.1038/nm.2693
8. Fu Y, Dominissini D, Rechavi G, He C. Gene expression regulation mediated through reversible m^{6}A RNA methylation. *Nat Rev Genet*. 2014;15:293–306. doi: 10.1038/nrg3724
9. Dominissini D, Moshitch-Moshkovitz S, Schwartz S, Salmon-Divon M, Ungar L, Osenberg S, Cesarkas K, Jacob-Hirsch J, Amariglio N, Kupiec M, Sorek R, Rechavi G. Topology of the human and mouse m6A RNA methylomes revealed by m6A-seq. *Nature*. 2012;485:201–206. doi: 10.1038/nature11112
10. Meyer KD, Saletore Y, Zumbo P, Elemento O, Mason CE, Jaffrey SR. Comprehensive analysis of mRNA methylation reveals enrichment in 3′ UTRs and near stop codons. *Cell*. 2012;149:1635–1646. doi: 10.1016/j.cell.2012.05.003
11. Batista PJ, Molinie B, Wang J, Qu K, Zhang J, Li L, Bouley DM, Lujan E, Haddad B, Daneshvar K, Carter AC, Flynn RA, Zhou C, Lim KS, Dedon P, Wernig M, Mullen AC, Xing Y, Giallourakis CC, Chang HY. m(6)A RNA modification controls cell fate transition in mammalian embryonic stem cells. *Cell Stem Cell*. 2014;15:707–719. doi: 10.1016/j.stem.2014.09.019
12. Geula S, Moshitch-Moshkovitz S, Dominissini D, Mansour AA, Kol N, Salmon-Divon M, Hershkovitz V, Peer E, Mor N, Manor YS, Ben-Haim MS, Eyal E, Yunger S, Pinto Y, Jaitin DA, Viukov S, Rais Y, Krupalnik V, Chomsky E, Zerbib M, Maza I, Rechavi Y, Massarwa R, Hanna S, Amit I, Levanon EY, Amariglio N, Stern-Ginossar N, Novershtern N, Rechavi G, Hanna JH. Stem cells. m6A mRNA methylation facilitates resolution of naïve pluripotency toward differentiation. *Science*. 2015;347:1002–1006. doi: 10.1126/science.1261417
13. Chen T, Hao YJ, Zhang Y, Li MM, Wang M, Han W, Wu Y, Lv Y, Hao J, Wang L, Li A, Yang Y, Jin KX, Zhao X, Li Y, Ping XL, Lai WY, Wu LG, Jiang G, Wang HL, Sang L, Wang XJ, Yang YG, Zhou Q. m(6)A RNA methylation is regulated by microRNAs and promotes reprogramming to pluripotency. *Cell Stem Cell*. 2015;16:289–301. doi: 10.1016/j.stem.2015.01.016
14. Fustin JM, Doi M, Yamaguchi Y, Hida H, Nishimura S, Yoshida M, Isagawa T, Morioka MS, Kakeya H, Manabe I, Okamura H. RNA-methylation-dependent RNA processing controls the speed of the circadian clock. *Cell*. 2013;155:793–806. doi: 10.1016/j.cell.2013.10.026
15. Wang Y, Li Y, Toth JI, Petroski MD, Zhang Z, Zhao JC. N6-methyladenosine modification destabilizes developmental regulators in embryonic stem cells. *Nat Cell Biol*. 2014;16:191–198. doi: 10.1038/ncb2902
16. Lin S, Choe J, Du P, Triboulet R, Gregory RI. The m(6)A methyltransferase METTL3 promotes translation in human cancer cells. *Mol Cell*. 2016;62:335–345. doi: 10.1016/j.molcel.2016.03.021
17. Oka T, Dai YS, Molkentin JD. Regulation of calcineurin through transcriptional induction of the calcineurin A beta promoter in vitro and in vivo. *Mol Cell Biol*. 2005;25:6649–6659. doi: 10.1128/MCB.25.15.6649-6659.2005
18. Simpson P, McGrath A, Savion S. Myocyte hypertrophy in neonatal rat heart cultures and its regulation by serum and by catecholamines. *Circ Res*. 1982;51:787–801.
19. Ackers-Johnson M, Li PY, Holmes AP, O'Brien SM, Pavlovic D, Foo RS. A simplified, Langendorff-free method for concomitant isolation of viable cardiac myocytes and nonmyocytes from the adult mouse heart. *Circ Res*. 2016;119:909–920. doi: 10.1161/CIRCRESAHA.116.309202
20. Mollova M, Bersell K, Walsh S, Savla J, Das LT, Park SY, Silberstein LE, Dos Remedios CG, Graham D, Colan S, Kühn B. Cardiomyocyte proliferation contributes to heart growth in young humans. *Proc Natl Acad Sci USA*. 2013;110:1446–1451. doi: 10.1073/pnas.1214608110
21. Zhang Y, Liu T, Meyer CA, Eeckhoute J, Johnson DS, Bernstein BE, Nusbaum C, Myers RM, Brown M, Li W, Liu XS. Model-based analysis of ChIP-Seq (MACS). *Genome Biol*. 2008;9:R137. doi: 10.1186/gb-2008-9-9-r137
22. Bardet AF, He Q, Zeitlinger J, Stark A. A computational pipeline for comparative ChIP-seq analyses. *Nat Protoc*. 2011;7:45–61. doi: 10.1038/nprot.2011.420
23. Thorvaldsdóttir H, Robinson JT, Mesirov JP. Integrative Genomics Viewer (IGV): high-performance genomics data visualization and exploration. *Brief Bioinform*. 2013;14:178–192. doi: 10.1093/bib/bbs017
24. Bass GT, Ryall KA, Katikapalli A, Taylor BE, Dang ST, Acton ST, Saucerman JJ. Automated image analysis identifies signaling pathways regulating distinct signatures of cardiac myocyte hypertrophy. *J Mol Cell Cardiol*. 2012;52:923–930. doi: 10.1016/j.yjmcc.2011.11.009
25. van Berlo JH, Maillet M, Molkentin JD. Signaling effectors underlying pathologic growth and remodeling of the heart. *J Clin Invest*. 2013;123:37–45. doi: 10.1172/JCI62839
26. Liu Q, Chen Y, Auger-Messier M, Molkentin JD. Interaction between NFκB and NFAT coordinates cardiac hypertrophy and pathological remodeling. *Circ Res*. 2012;110:1077–1086. doi: 10.1161/CIRCRESAHA.111.260729
27. Bogoyevitch MA, Sugden PH. The role of protein kinases in adaptational growth of the heart. *Int J Biochem Cell Biol*. 1996;28:1–12.
28. Li J, Kritzer MD, Michel JJ, Le A, Thakur H, Gayanilo M, Passariello CL, Negro A, Danial JB, Oskouei B, Sanders M, Hare JM, Hanauer A, Dodge-Kafka K, Kapiloff MS. Anchored p90 ribosomal S6 kinase 3 is required for cardiac myocyte hypertrophy. *Circ Res*. 2013;112:128–139. doi: 10.1161/CIRCRESAHA.112.276162
29. Jia G, Fu Y, Zhao X, Dai Q, Zheng G, Yang Y, Yi C, Lindahl T, Pan T, Yang YG, He C. N6-methyladenosine in nuclear RNA is a major substrate of the obesity-associated FTO. *Nat Chem Biol*. 2011;7:885–887. doi: 10.1038/nchembio.687
30. Liu J, Yue Y, Han D, Wang X, Fu Y, Zhang L, Jia G, Yu M, Lu Z, Deng X, Dai Q, Chen W, He C. A METTL3-METTL14 complex mediates mammalian nuclear RNA N6-adenosine methylation. *Nat Chem Biol*. 2014;10:93–95. doi: 10.1038/nchembio.1432
31. Ping XL, Sun BF, Wang L, Xiao W, Yang X, Wang WJ, Adhikari S, Shi Y, Lv Y, Chen YS, Zhao X, Li A, Yang Y, Dahal U, Lou XM, Liu X, Huang J, Yuan WP, Zhu XF, Cheng T, Zhao YL, Wang X, Rendtlew Danielsen JM, Liu F, Yang YG. Mammalian WTAP is a regulatory subunit of the RNA N6-methyladenosine methyltransferase. *Cell Res*. 2014;24:177–189. doi: 10.1038/cr.2014.3
32. Fedeles BI, Singh V, Delaney JC, Li D, Essigmann JM. The AlkB Family of Fe(II)/α-ketoglutarate-dependent dioxygenases: repairing nucleic acid alkylation damage and beyond. *J Biol Chem*. 2015;290:20734–20742. doi: 10.1074/jbc.R115.656462
33. Wang X, He C. Reading RNA methylation codes through methyl-specific binding proteins. *RNA Biol*. 2014;11:669–672.
34. Liu N, Pan T. RNA epigenetics. *Transl Res*. 2015;165:28–35. doi: 10.1016/j.trsl.2014.04.003
35. de Nadal E, Ammerer G, Posas F. Controlling gene expression in response to stress. *Nat Rev Genet*. 2011;12:833–845. doi: 10.1038/nrg3055
36. Kehat I, Davis J, Tiburcy M, Accornero F, Saba-El-Leil MK, Maillet M, York AJ, Lorenz JN, Zimmermann WH, Meloche S, Molkentin JD. Extracellular signal-regulated kinases 1 and 2 regulate the balance between eccentric and concentric cardiac growth. *Circ Res*. 2011;108:176–183. doi: 10.1161/CIRCRESAHA.110.231514